

A Highly Efficient, Preorganized Macrobicyclic Receptor for Halides Based on CH \cdots and NH \cdots Anion Interactions

Christos A. Ilioudis,[†] Derek A. Tocher,[‡] and Jonathan W. Steed^{*,§}

Contribution from the Department of Chemistry, King's College London, Strand, London, WC2R 2LS, U.K., Department of Chemistry, University College London, 20 Gordon Street, London WC1H 0AJ, and Department of Chemistry, University of Durham, University Science Laboratories, South Road, Durham, DH1 3LE, U.K.

Received May 19, 2004; E-mail: jon.steed@durham.ac.uk

Abstract: The preorganized, macrobicyclic azaphane (**1**) exhibits remarkable strong, selective fluoride binding comparable to the most effective bis(tren) cryptands despite binding anions via only three NH groups coupled with three CH hydrogen bond donors. The lower intrinsic affinity of CH donors is compensated by the high degree of preorganization exhibited by azacyclophane **1**. Compound **1** is prepared via a tripod–tripod cyclization reaction between 1,3,5-tris-bromomethyl-benzene and an aliphatic tripodal hexatosylated polyamine, followed by the reduction of the resulting bicyclic tosylamine. The crystal structures of the bicyclic tosylamine **2** and four macrobicyclic polyammonium halide salts of **1** are reported. X-ray studies revealed the formation of inclusive 1:1 complexes of **1** with fluoride, chloride, bromide, and iodide. Potentiometric titrations showed very high binding constants for fluoride and chloride with a F⁻/Cl⁻ selectivity of more than five logarithmic units. The final geometry of the anion cryptates is largely determined by optimization of NH and CH \cdots anion interactions coupled with unfavorable anion– π repulsion for the larger anions.

Introduction

Anion coordination chemistry¹ is one of the most topical and challenging areas of current research within supramolecular chemistry.^{2,3} The field includes exciting current work in the binding and transport of nucleotides^{4,5} and amino acids,^{6,7} along with applications in catalysis,⁸ analytical chemistry,^{9,10} and anion-templated reactions.^{11–13}

Various types of receptors have been synthesized and used as complexones for anionic species in the past 35 years.¹⁴

Polyammonium macrobicycles constitute one of the most successful and widely used classes of molecules for anion binding.^{15,16} Hosts such as the octaazacryptand (OAC) and bis-(tren) (BT, Figure 1) have been reported by Dietrich et al. to show very high binding constants for halide species. In the hexaprotonated form, the small cryptand OAC has a very large log K_s value of 10.55 for fluoride¹⁷ (or 11.2¹⁸) whereas BT has log K_s values of 4.10 and 3.00 for fluoride and chloride, respectively.¹⁹ It was proposed that the preorganized array of six NH⁺ donors in protonated OAC is highly complementary to F⁻. It is remarkable, however, that the ligand BT also potentially presents six NH groups in a preorganized array and yet is so much less effective at binding fluoride, despite the comparable affinity for chloride. The larger cryptands have an affinity for larger anions such as CrO₄²⁻.^{20,21}

In our previous crystallographic studies of aliphatic polyammonium halide salts,²² we noted a preference for halide species toward the adoption of trigonal coordination environments in

[†] King's College London.

[‡] University College London.

[§] University of Durham.

- (1) Bianchi, A.; Bowman-James, K.; Garcia-Espana, E. *Supramolecular Chemistry of Anions*; Wiley-VCH: New York, 1997.
- (2) Lehn, J.-M. *Supramolecular Chemistry*, 1st ed.; VCH: Weinheim, Germany, 1995; p 271.
- (3) Steed, J. W.; Atwood, J. L. *Supramolecular Chemistry*; Wiley: Chichester, U.K., 2000.
- (4) Adams, R. L. P.; Knowler, J. T.; Leader, D. P. *The Biochemistry of the Nucleic Acids*; Chapman and Hall: New York, 1986.
- (5) Wirth, W.; Blotvogel-Baltronat, J.; Kleinkes, U.; Sheldrick, W. S. *Inorg. Chim. Acta* **2002**, *339*, 14–26.
- (6) Kyne, G. M.; Light, M. E.; Hursthouse, M. B.; de Mendoza, J.; Kilburn, J. D. *J. Chem. Soc., Perkin Trans. 1* **2001**, 1258–1263.
- (7) Wehner, M.; Schrader, T. *Angew. Chem., Int. Ed.* **2002**, *41*, 1751–1754.
- (8) Lehn, J.-M. *Supramolecular Reactivity and Catalysis of Phosphoryl Transfer*. In *Bioorganic Chemistry in Healthcare and Technology*; Pandit, U. K., Alderweireldt, F. C., Eds.; Plenum Press: New York, 1991.
- (9) Snyder, L. R.; Glajch, J. L.; Kirkland, J. J. *Practical HPLC Method Development*; Wiley & Sons: New York, 1988.
- (10) Schmidtchen, F. P. *Nachr. Chem. Tech. Lab.* **1988**, *36*, 8–12.
- (11) Yang, X.; Knobler, C. B.; Hawthorne, M. F. *Angew. Chem., Int. Ed. Engl.* **1991**, *30*, 1507–1508.
- (12) Zeng, Z.; Yang, X.; Knobler, C. B.; Hawthorne, M. F. *J. Am. Chem. Soc.* **1993**, *115*, 5320–5321.
- (13) Zeng, Z.; Knobler, C. B.; Hawthorne, M. F. *J. Am. Chem. Soc.* **1995**, *117*, 5105–5113.

(14) Schmidtchen, F. P.; Berger, M. *Chem. Rev.* **1997**, *97*, 1609–1646.

(15) Ilioudis, C. A.; Steed, J. W. *J. Supramol. Chem.* **2001**, *1*, 165–187.

(16) Llinares, J. M.; Powell, D.; Bowman-James, K. *Coord. Chem. Rev.* **2003**, *240*, 57–75.

(17) Dietrich, B.; Dilworth, B.; Lehn, J.-M.; Souchez, J.-P.; Cesario, M.; Guilhem, J.; Pascard, C. *Helv. Chim. Acta* **1996**, *79*, 569–587.

(18) Reilly, S. D.; Khalsa, G. R. K.; Ford, D. K.; Brainard, J. R.; Hay, B. P.; Smith, P. H. *Inorg. Chem.* **1995**, *34*, 569–575.

(19) Dietrich, B.; Guilhem, J.; Lehn, J.-M.; Pascard, C.; Sonveaux, E. *Helv. Chim. Acta* **1984**, *67*, 91–104.

(20) Maubert, B. M.; Nelson, J.; McKee, V.; Town, R. M.; Pål, I. *J. Chem. Soc., Dalton Trans.* **2001**, 1395–1397.

(21) McKee, V.; Nelson, J.; Town, R. M. *Chem. Soc. Rev.* **2003**, *32*, 309–325.

(22) Ilioudis, C. A.; Hancock, K. S. B.; Georganopoulou, D. G.; Steed, J. W. *New J. Chem.* **2000**, *24*, 787–798.

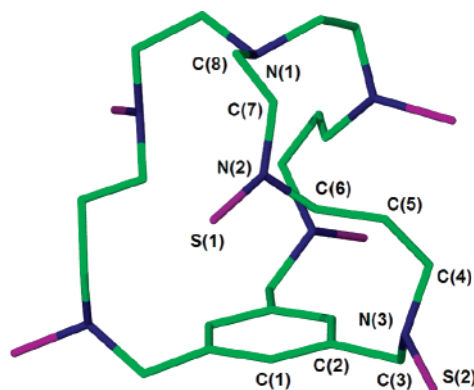


Figure 2. X-ray crystal structure of **2**. All atoms belonging to the tosyl moieties have been removed for the sake of clarity with the exception of sulfur atoms.

synthesis of compound **8** proceeded under satisfactory yields, but the macrobicyclization afforded only 19% of the tosylamine **2**. Detosylation of **2** afforded the target compound in good yield.

All new compounds were characterized by the usual analytical and spectroscopic techniques (see Experimental Section). The structure of the hexatosylate **2** was determined by X-ray crystallography to provide information about the degree of preorganization of the receptor in the absence of protonation or anionic guest species. Suitable crystals for X-ray diffraction for **2** were grown by slow diffusion of pentane in a concentrated solution of the product in dichloromethane. The aliphatic portion of the tosylated macrobicyclic is clearly preorganized for the intracavity binding of a halide anion (Figure 2), exhibiting an *in*²⁸ conformation of the apical nitrogen atom. The distance from the apical N atom to the aromatic ring centroid is relatively short in comparison to the analogous halide complexes (vide infra, N \cdots centroid distance 5.872(19) Å), consistent with minimization of free cavity volume. This contraction has the effect of splaying out the lower (benzylic) amine nitrogen atoms (N \cdots N distances 6.408 Å, C₃ symmetric) in a fashion unsuitable for convergent guest binding. The methylenic chains are, however, appropriately positioned to interact with a potential guest species. It would be anticipated that upon protonation the cavity would enlarge as a consequence of repulsions between the protonated amine nitrogen atoms, resulting in an increase of the N_{apical} \cdots centroid distance and a decrease of the helical twist angle (taken as the N(1)–N(2)–N(3)–C(2) torsion angle, 59.1° in **2**) of the C₃ chiral, propeller-like conformation.

Hydrohalide Salts of Compound 1. It has proved possible to crystallize compound **1** in the presence of fluoride, chloride, bromide, and iodide from an aqueous solution of the corresponding haloacid by slow evaporation. A mixed fluoride/silicon hexafluoride hydrate salt (**1**·2HF·2H₂SiF₆·7H₂O) resulted from crystallization with hydrofluoric acid, presumably as a result of glass corrosion. The chloride complex also crystallized as a hydrate **1**·6HCl·4H₂O. The polyiodide salt **1**·2HI·4HI₃ was obtained from hydroiodic acid, with the I₃[−] arising from partial aerobic iodide oxidation. In the case of fluoride, chloride, and

iodide, the macrobicyclic crystallized in its hexaprotonated form, whereas the bromide salt **1**·7HBr·3H₂O involved a heptaprotonated cryptand. Importantly, in all four cases, a halide anion is located inside the cavity of the macrobicyclic. Key structural parameters are given in Table 1. Crystallographic parameters for the new macrobicyclic systems are given in Table 2.

The most striking feature of the structures of protonated **1** is the significant lengthening of the host cavity (as exemplified by the N_{apical} \cdots centroid distance, Table 1) compared to the precursor **2**, along with a corresponding decrease in the helical twist angle. Thus the main conformational change on protonation and anion complexation comprises a facile lengthening and concomitant untwisting of the macrobicyclic. Surprisingly, this effect is most marked for the smallest anion, F[−] which exhibits the longest N_{apical} \cdots centroid distance of 7.52 Å. The structural similarity between the fluoride complex of **1**·6H⁺ and the hexaprotonated OAC is marked (Figure 4), with CH₂ groups from both the end of the propylenic chains (C8 and C20) and even the middle (C15) all interacting²⁹ with the included fluoride anion in a fashion similar to the NH moieties in the OAC cryptate (Figure 3). OAC displays the largest binding constants known for fluoride.¹⁷ The average N \cdots F[−] distance for the complexed fluoride in the case of OAC is 2.835 Å, whereas the corresponding distance for cryptand **1** is 2.648(3) Å, suggesting a very good match between the cavity of the newly synthesized cryptand and fluoride anion and displacement of the anion toward the NH donors and away from the weaker hydrogen bonding CH sites (hydrogen bond distances: N(4) \cdots F(1): 2.679(3) Å, N(5) \cdots F(1): 2.619(3) Å, N(6) \cdots F(1): 2.646(3) Å, C(8) \cdots F(1): 3.414(3) Å, C(15) \cdots F(1): 3.356(3) Å, C(20) \cdots F(1): 3.297(3) Å). The lower NH₂⁺ groups hydrogen bond with anions outside the cavity. The other halide anions Cl[−] to I[−] are all held in a similar fashion, with three NH \cdots X[−] and three CH \cdots X[−] hydrogen bonds completing a *pseudo*-octahedral coordination about each halide guest (Figure 4). Hydrogen bond distances increase approximately in proportion to the anion ionic radii. As in the fluoride case, the overall Cl[−] binding environment, distorted octahedral, is once more very similar to the one observed for the corresponding hexaprotonated octaazacryptand OAC·6HCl·2.75H₂O.³⁰ In the case of **1**·6HCl·4.5H₂O, and despite less competition for chloride binding from a second set of NH groups, the average N \cdots Cl[−] distance for the newly synthesized complex is 3.164(8) Å, slightly larger than that observed in OAC·6HCl·2.75H₂O (3.085 Å), probably indicative of a better match between the cavity of OAC and chloride than between the cavity of **1** and chloride, at least in the solid state. In the bromide case, there are two conformationally very different independent molecules (Figure 4b and c). Both exhibit a short NH_{apical} \cdots Br[−] interaction because the cryptand is heptaprotonated, but the resulting strain is apparently sufficient to destabilize the convergent geometry of the three tren secondary ammonium groups and allow the formation of a conformer with an NH₂⁺ group pointing out of the cavity. Thus, one intracavity bromide ion exhibits a CH \cdots Br[−] interaction instead of an NH⁺ \cdots Br[−] hydrogen bond (Figure 4c). The other conformer exhibits the more conventional

(23) Heyer, D.; Lehn, J. M. *Tetrahedron Lett.* **1986**, 27, 5869–5872.

(24) Ilioudis, C. A.; Bearpark, M. J.; Steed, J. W. Unpublished work, 2004.

(25) Dietrich, B.; Hosseini, M. W.; Lehn, J.-M.; Sessions, R. B. *Helv. Chim. Acta* **1985**, 68, 289–299.

(26) Dietrich, B.; Lehn, J.-M.; Sauvage, J. P.; Blanzat, J. *Tetrahedron* **1973**, 29, 1629–1645.

(27) Illuminati, G.; Mandolini, L. *Acc. Chem. Res.* **1981**, 14, 95–102.

(28) Park, C. H.; Simmons, H. E. *J. Am. Chem. Soc.* **1968**, 90, 2431–2433.

(29) Desiraju, G. R.; Steiner, T. *The Weak Hydrogen Bond in Structural Chemistry and Biology*; Oxford University Press: Oxford, 1999; p 480.

(30) Hossain, M. A.; Linares, J. M.; Miller, C. A.; Seib, L.; Bowman-James, K. *Chem. Commun.* **2000**, 2269–2270.

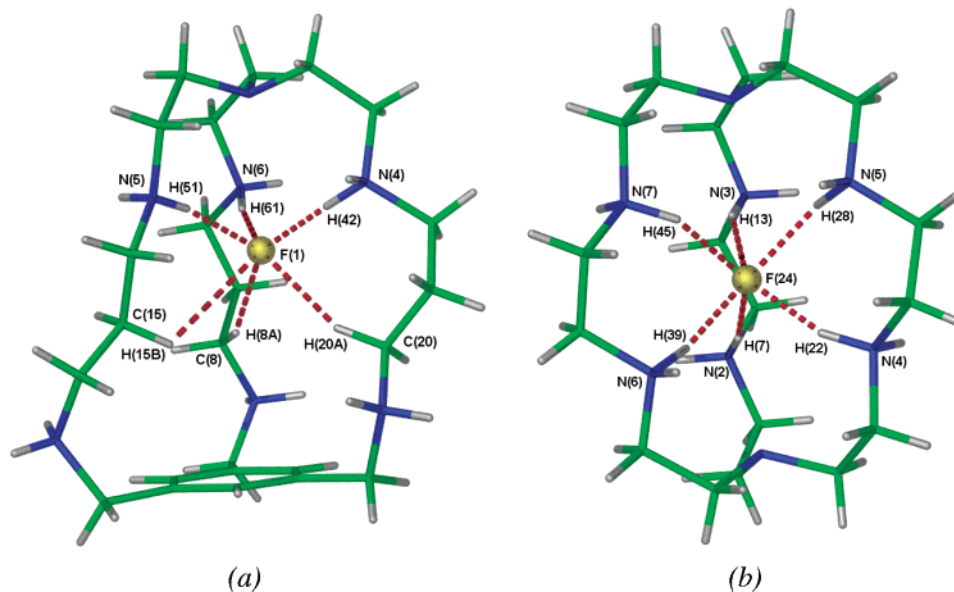
Table 1. Structural Data for the Cryptates Reported in the Present Work^a

	compound				
	1·2HF·2H ₂ SiF ₆ ·7H ₂ O	1·6HCl·4H ₂ O	1·7HBr·3H ₂ O	1·2HI·4HI ₃	2
N _{apex} ···X ⁻ (Å)	3.066(3)	3.445(7)	3.169(12)	3.786(13)	—
cntr···X ⁻ (Å)	4.506(3)	3.652(8)	3.653(14)	3.692(13)	—
N _{apex} ···cntr (Å)	7.520(4)	7.169(11)	6.804(19)	7.468(18)	5.872(19)
helical twist angle (deg) ^b	20.5–31.8	10.6–29.4	9.0–36.0	9.0–28.7	59.1
		6.3–13.9	1.9–63.2 ^c		

^a Data for the tosylated precursor **2** are included for comparison. N_{apex} refers to the apical nitrogen atom of the ligand, X⁻ refers to the corresponding halide anion inside the cavity of the cryptand, and “cntr” (centroid) refers to the point that corresponds to the center of the aromatic ring of the cryptand.
^b The helical twist angle is defined as the N_{apical}–NH₂–NH₂–C_{aryl} torsion angle. The values for two crystallographically unique cryptates for the chloride and the bromide salts are given. ^c Disordered.

Table 2. Crystallographic Parameters for New Macrocyclic Systems

	2	1·2HF·2H ₂ SiF ₆ ·7H ₂ O	1·6HCl·4.5H ₂ O	1·7HBr·3H ₂ O	1·2HI·4HI ₃
formula	C ₆₉ H ₈₇ Cl ₆ N ₇ O ₁₂ S ₆	C ₂₄ H ₆₅ F ₁₄ N ₇ O ₇ Si ₂	C ₂₄ H ₆₀ Cl ₆ N ₇ O _{4.5}	C ₂₄ H ₅₈ Br ₇ N ₇ O ₃	C ₂₄ H ₅₁ I ₁₄ N ₇
M	1611.61	885.97	731.51	1052.10	2214.32
system	rhombohedral	monoclinic	triclinic	monoclinic	triclinic
space group	R3	P2 ₁ /n	P1̄	P1̄	P1̄
a/Å	16.3404(23)	14.0345(9)	11.2494(8)	11.2538(4)	11.4033(12)
b/Å		15.9137(10)	16.2958(12)	18.0137(8)	11.5662(12)
c/Å	28.0178(27)	17.6318(11)	21.1945(19)	20.9088(8)	21.966(2)
α/deg			78.3122(27)	74.548(3)	85.670(2)
β/deg		96.2392(45)	85.1281(32)	82.221(2)	83.181(2)
γ/deg			82.6143(40)	73.058(3)	61.557(2)
V/Å ³	6479.0(18)	3914.6(14)	3719.3(13)	3900.5(14)	2528.8(5)
Z	3	6	2	2	2
No. msd. rflns	10 189	13 422	43 774	24 842	20 906
No. un. rflns	5656	7845	13 301	15 500	11 340
R1 (on F, I > 2σ(I))	0.2118	0.0550	0.1420	0.1135	0.0756
wR2 (on F ² , all data)	0.3388	0.1405	0.3553	0.2951	0.1956

**Figure 3.** Encapsulation of a fluoride anion (a) in the crystal structure of 1·2HF·2H₂SiF₆·7H₂O and (b) in the crystal structure of OAC·3HF·HCl·2SiF₆·5H₂O. The similarities between the ligand conformations and the coordination geometries of the included anions are evident.

three NH···Br⁻ and three CH···Br⁻ short contacts in addition to the apical interaction with C···Br⁻ distances between 3.644(17) and 3.936(14) Å, typical for this kind of interaction. It is useful to make a comparison between this structure and other structures of protonated tren units with bromide anions.²² In the case of the monoprotonated tren monobromide, a clear chelate effect was observed for the tren unit, with unprotonated secondary amine units as well as the ammonium group

interacting with the anion. In contrast, the tetraprotonated tren tetrabromide displays no chelate effect at all, probably because of the mutual repulsion among the ammonium moieties. Moving to the iodide case, N···I⁻ distances for the ammonium moieties of the tren unit are 3.427(13), 3.441(13), and 3.479(13) Å. Again, three C–H···I⁻ weak interactions complete the coordination sphere of the complexed iodide (Figure 4d) with C···I⁻ distances at 3.620(15), 3.728(13), and 3.740(15) Å.

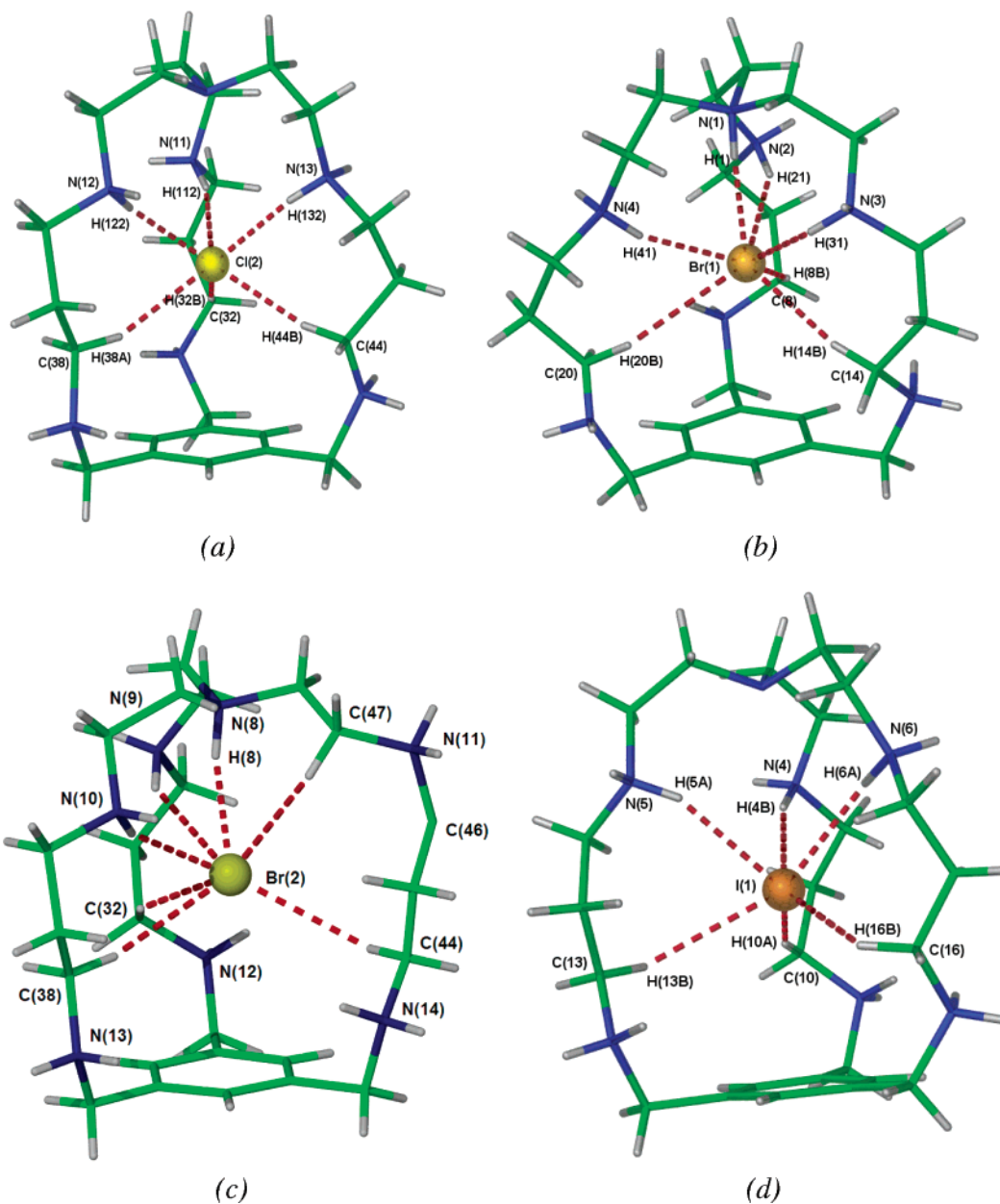


Figure 4. Encapsulation of (a) a chloride anion in the crystal structure of $1 \cdot 6\text{HCl} \cdot 4.5\text{H}_2\text{O}$ and (b, c) bromide in $1 \cdot 7\text{HBr} \cdot 3\text{H}_2\text{O}$, two conformationally different independent molecules. An additional $\text{NH}^+ \cdots \text{Br}^-$ hydrogen bond in each case is formed because the cryptand is heptaprotonated with $N_{\text{apical}} \cdots \text{Br}^-$ distances of 3.169(12) Å and 3.187(14) Å. Disordered H atoms on C46 not shown. (d) Iodide anion in the crystal structure of $1 \cdot 2\text{HI} \cdot 4\text{HI}_3$. Smaller “bite” angles are observed as a result of the positioning of the encapsulated iodide further away from the apical nitrogen atom.

Interestingly, the fluoride salt exhibits a rather long anion \cdots centroid separation of 4.506 Å, a parameter that remains remarkably constant at ca. 3.6 Å for all of the other anions (Table 1), including both symmetry-independent molecules in the case of the Cl^- and Br^- analogues. The fact that this rather short distance does not increase with increasing halide size suggests that the halide anions are in repulsive contact with the aromatic ring and hence suggests that the binding of all halides except F^- should consequently be destabilized. This observation is borne out by potentiometric titration data (vide infra). The flexibility of the aliphatic end of the molecule is exemplified in the consistent increase in the $N_{\text{apical}} \cdots \text{X}^-$ distance from 3.06 Å in the fluoride case to 3.78 Å in the iodide case. The exception to this rule is the bromide salt, which would be expected to exhibit a short $N_{\text{apical}} \cdots \text{Br}^-$ distance because the apical nitrogen

atom is protonated, in contrast to all of the other structures, and hence an additional $\text{NH}_{\text{apical}} \cdots \text{Br}^-$ hydrogen bond is formed. The effects of the proximity of the aromatic ring on the overall length of the cryptand ($N_{\text{apical}} \cdots$ centroid distances, Table 1) contrast with the relatively minor changes observed in related systems. For example, in the case of OAC the apical $\text{N} \cdots \text{N}$ distance is 6.60 Å for the chloride complex²⁴ and 6.65 Å for the fluoride complex.¹⁷ The cavity dimensions for the “Bis-Tren” fluoride, chloride, and bromide complexes are 7.66 and 8.02 Å (two crystallographically unique ligands), 7.40, and 7.50 Å, respectively.¹⁹

The locations of the extracavity anions are shown for the SiF_6^{2-} and I_3^- species in Figure 5. The anions approach each one of the sides of the approximately C_3 symmetric cryptate, interacting with the tren NH_2^+ units via bifurcated $\text{NH} \cdots \text{F}$

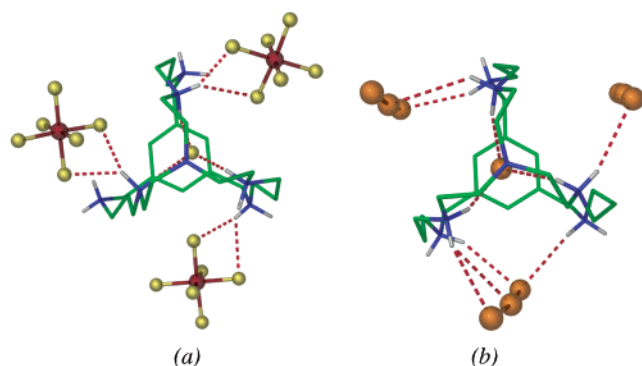


Figure 5. Packing of extracavity anions in the crystal structure of (a) $1 \cdot 2\text{HF} \cdot 2\text{H}_2\text{SiF}_6 \cdot 7\text{H}_2\text{O}$ and (b) $1 \cdot 2\text{HI} \cdot 4\text{HI}_3$.

hydrogen bonds in the case of SiF_6^- ($\text{N} \cdots \text{F}$ distances 2.726–3.101(3) Å) and $\text{NH} \cdots \text{I}$ interactions for I_3^- . Similar packing is observed for the chloride and bromide analogues, and in all cases additional $\text{CH} \cdots \text{X}^-$ weaker interactions are also formed between the cryptand and the extracavity anions.

Solution Studies. The protonation constants for **1** were determined potentiometrically and are shown in Table 3. These values are not very different from protonation constants measured for other azaphane cryptands such as *m*-BTC and *p*-BTC (Figure 1), as well as a series of related cryptands.³¹ It seems that the existence of propylene units balances a greater loss of basicity expected because of mutual Coulombic repulsion and the existence of the aromatic unit. The first three protonation constants presumably represent the $\text{p}K_a$ values of the amine moieties of the tren unit, and indeed they are close to the corresponding values for tren itself. The benzylic NH groups are more difficult to protonate because of the delocalization of the amine lone pair into the aryl ring.³² The last protonation constant presumably corresponds to the apical nitrogen, which remains unprotonated in most of the systems studied in this work, and is similar to that found for tren itself under the same experimental conditions.

The protonation behavior of this ligand was also studied in the presence of 0.01 M TsOH/0.1 M TsONa. The tosylate anion was chosen because it is unlikely to bind with the macrocyclic cavity of **1**. With the exception of the first basicity constant, all other basicity constants were found to be smaller than those observed in the presence of 0.01 M HNO_3 /0.1 M NaNO_3 , and the last protonation constant was not apparently accessible under the experimental conditions. The NO_3^- anion (and other smaller hydrogen bond acceptor anions by implication) apparently has a significant role in stabilizing higher protonated species.

The anion binding stability constants of ligand **1** were investigated in the presence of 0.01 M TsOH and 0.1 M TsONa as supporting electrolyte. pH titrations were conducted in the presence of excess of NaF, NaCl, NaBr, and NaNO_3 . Essentially no change of the titration curve was observed in the titration of **1** in the presence of NaBr or NaNO_3 compared to the reference measurement, suggesting very low binding constants. First stability constants for F^- and Cl^- are shown in Table 4 for various protonated species.

The pH titration data are consistent with crystal structures for the fluoride and chloride complexes. In fact, remarkably high binding constants, consistent with the formation of a 1:1 inclusion complex, are observed in the presence of excess of fluoride anion (Table 4). Significantly lower binding constants were observed for chloride, comparable to those obtained for the small octaazacryptand (Figure 1), and $1 \cdot 6\text{H}^+$ exhibits a marked F^-/Cl^- selectivity ($>10^5$), again paralleling OAC.^{17,18} The high fluoride affinity and F^-/Cl^- selectivity observed for **1** are remarkable in that, as shown crystallographically, F^- complexation occurs via only three NH moieties, reinforced by interactions with three CH_2 groups. The clear implication is that the preorganization of the host system is a significantly more important factor than the nature of the binding groups.

Although potentiometric and X-ray diffraction studies are in agreement and consistent with the formation of intracavity complexes in the case of F^- and Cl^- , no binding is observed for Br^- or NO_3^- anions. The weak binding of Br^- in particular is surprising given that this anion (and I^-) is included in the cavity in the solid state; however, it is likely that inclusion of larger halides introduces significant strain and hence destabilizes solution binding, particularly involving unfavorable anion $\cdots\pi$ interactions. The fact that intracavity inclusion of the larger halide anions is observed crystallographically can be traced to the conditions under which compound **1** was crystallized in the presence of hydrobromic or hydroiodic acid. Concentrated acidic solutions were used for crystallization experiments resulting, in the case of the bromide complex, in a heptaprotonated host and in both cases very high effective concentrations of halide anions. This phenomenon was also investigated in the case of OAC.³⁰ An inclusive complex with chloride was obtained by treatment with concentrated hydrochloric acid despite the fact that earlier work suggested an enormous F^-/Cl^- selectivity of more than eight logarithmic units for this cryptand. The workers investigated the affinity patterns of this cryptand by NMR techniques and concluded that it displays a dramatic enhancement of its affinity for chloride below pH 2.5. It is likely that compound **1** is subjected to the same effect at low pH, forming cryptate complexes with both bromide and iodide. The origins in this shift in selectivity may well be explicable in terms of protonation of the apical tertiary amine nitrogen atom, introducing an additional $\text{NH}^+ \cdots \text{X}^-$ hydrogen bond as observed in the crystal structure of $1 \cdot 7\text{HBr} \cdot 3\text{H}_2\text{O}$. This behavior cannot be studied by pH titrations because conventional potentiometric techniques employed are only generally considered to be accurate over a pH range of 2.5–11.

Experimental Section

Materials. The starting materials were obtained in the highest purity available and used without further purification.

NMR Spectra. ^1H and ^{13}C NMR spectra at room temperature were measured with a Bruker Avance NMR spectrometer, operating at 360 and 90 MHz, respectively, and the chemical shifts are reported in parts per million relative to tetramethylsilane.

Mass Spectra. Fast atom bombardment (low resolution) mass spectra were obtained with a Kratos MS 890 mass spectrometer. High-resolution mass spectra were obtained with a Bruker Apex III mass spectrometer by electrospray ionization.

Elemental Analysis. Elemental analysis for carbon, hydrogen, and nitrogen was carried out by the Elemental Analysis Service at the London Metropolitan University.

(31) Arnaud-Neu, F.; Fuangwasdi, S.; Maubert, B.; Nelson, J.; McKee, V. *Inorg. Chem.* **2000**, *39*, 573–579.

(32) Bencini, A.; Bianchi, A.; Garcia-Espana, E.; Micheloni, M.; Ramirez, J. A. *Coord. Chem. Rev.* **1999**, *188*, 97–156.

Table 3. Logarithms of the Stepwise Protonation Constants for *meta*-Cyclophane **1**^a

	log K_1	log K_2	log K_3	log K_4	log K_5	log K_6	log K_7	log K_8
1 ^b	9.50(16)	9.82(7)	8.47(7)	7.61(10)	7.18(10)	6.75(6)	2.37(10)	51.70(66)
1 ^c	9.58(19)	9.50(11)	7.90(12)	6.85(11)	4.99(9)	3.19(10)	—	42.01(72)
BT ^d	9.99	9.02	7.98	7.20	6.40	5.67	—	46.26
OAC ^e	11.2	9.4	7.6	5.78	4.4	—	—	38.38

^a Values for BT and OAC (Figure 1) are included for comparison. ^b 0.001 M ligand **1**, 0.01 M HCl, 0.1 M NaNO₃. ^c 0.001 M ligand **1**, 0.01 M TsOH, 0.1 M TsONa. ^d 0.1 M NaClO₄ taken from ref 32. ^e 0.1 M KNO₃ log K_5 is a two-proton step, taken from ref 32.

Table 4. First Anion Binding Constants Observed for Ligand **1** at Different States of Protonation^a

species	log K_1			
	F ⁻	Cl ⁻	Br ⁻	NO ₃ ⁻
1 ·H ₆ X	9.54(12)	4.19(13)	—	—
1 ·H ₅ X	7.84(8)	3.88(9)	—	—
1 ·H ₄ X	5.65(12)	2.06(26)	—	—
1 ·H ₃ X	4.86(9)	—	—	—

^a The acid dissociation constant (log $K = 3.25$) for HF was included in the calculations. Values for bromide and nitrate were apparently too small to measure.

Potentiometric Titrations. All potentiometric titrations were performed at room temperature, using carbonate-free NaOH with a Titrimo model 736 GP along with a Metrohm combined glass electrode. The protonation constants were determined from titrations of an approximately 10⁻³ M ligand solution containing an excess of HNO₃ or TsOH (typically 0.01 M) in the presence of NaNO₃ or TsONa to maintain ionic strength at 0.1 M. Anion binding constants for anionic species X⁻ were determined from titrations of an approximately 10⁻³ M ligand solution containing excess of TsOH (0.01 M or more) in the presence of approximately 0.01 M of the corresponding salt NaX, and TsONa (0.1 M) to maintain ionic strength at 0.1 M. The range of accurate pH measurements was considered to be 2.5–11. Stability constants were calculated with the program HYPERQUAD.³³

X-ray Crystallography. Crystal data and data collection parameters are summarized in Table 1. Crystals were mounted using silicon grease on a thin glass fiber. All crystallographic measurements (except in the case of **1**·2HI·4HI₃) were carried out with a Nonius Kappa CCD diffractometer equipped with graphite monochromated Mo K α radiation using wide ϕ - and ω -scans. Data collection temperature was 120 K, maintained by using an Oxford Cryosystem low-temperature device. Integration was carried out by the Denzo-SMN package.³⁴ Data sets were corrected for Lorentz and polarization effects and for the effects of absorption (Scalepack)³⁴ and crystal decay where appropriate. Structures were solved using the direct methods option of SHELXS-97³⁵ and developed using conventional alternating cycles of least-squares refinement (SHELXL-97)³⁶ and difference Fourier synthesis with the aid of the program XSeed.³⁷ In all cases, non-hydrogen atoms were refined anisotropically except for some disordered atoms, while C–H hydrogen atoms were fixed in idealized positions and allowed to ride on the atom to which they were attached. Hydrogen atom thermal parameters were tied to those of the atom to which they were attached. Where possible, acidic hydrogen atoms were located experimentally, and their positional and isotropic displacement parameters were refined. All calculations were carried out on an IBM-PC compatible personal computer.

In the crystal structure of **1**·6HCl·4.5H₂O, chloride atoms Cl(7), Cl(9), Cl(10), and Cl(13) were disordered and given half occupancy each.

(33) Gans, P.; Sabatini, A.; Vacca, A. *Talanta* **1996**, *43*, 1739–1753.

(34) Otwinowski, Z.; Minor, W. *Methods in Enzymology*; Carter, C. W., Sweet, R. M., Eds.; Academic Press: London, 1997; Vol. 276, pp 307–326.

(35) Sheldrick, G. M. *SHELXS-97*, University of Göttingen: Göttingen, Germany, 1997.

(36) Sheldrick, G. M. *SHELXL-97*, University of Göttingen: Göttingen, Germany, 1997.

(37) Barbour, L. J. *J. Supramol. Chem.* **2001**, *1*, 189–191.

In the crystal structure of **1**·7HBr·3H₂O, bromide atoms Br(4), Br(5), Br(7), Br(8), Br(9), Br(10), Br(17), and Br(18) were disordered and given half occupancy each.

The relatively poor precision of the structures of **1**·6HCl·4.5H₂O, **1**·7HBr·3H₂O, and **2** arises principally from sample quality issues. Crystals of these large unit cells, solvated systems proved in general to be small, to be of high mosaicity, and to exhibit a marked tendency toward formation of multiple, fused crystallites. In each case, a number of samples were examined with an emphasis on obtaining a crystal as nearly single as possible. In the case of **1**·6HCl·4.5H₂O and **1**·7HBr·3H₂O, the problems are increased by disorder and absorption issues. However, the overall atom positions are clear and unambiguous, particularly the location of the intracavity anion.

The crystal structure of **1**·2HI·4HI₃ was obtained using a Bruker SMART APEX CCD diffractometer using graphite-monochromated Mo K α radiation ($\lambda = 0.71073$ Å) at 298 ± 2 K. Data reduction and integration were carried out with SAINT+, and absorption corrections were applied using the program SADABS. Structures were solved by direct methods and developed using alternating cycles of least-squares refinement and difference Fourier synthesis. All non-hydrogen atoms were refined anisotropically. Hydrogen atoms were placed in calculated positions, and their thermal parameters were linked to those of the atoms to which they were attached (riding model). For structure solution and refinement, we used the SHELXTL PLUS V6.10 program package.

Synthesis. Trimethyl-1,3,5-Benzenetricarboxylate (3). Benzenetricarboxylic acid (10.0 g, 47.5 mmol), methanol (200 mL), and concentrated sulfuric acid (2.5 mL) were mixed and then refluxed for 24 h. The solvent was evaporated, and the residue was dissolved in chloroform (200 mL) and then washed with a saturated solution of potassium carbonate (250 mL). The solvent was removed under reduced pressure to afford **3** as a white powder (10.91 g, 92%).

¹H NMR (CDCl₃): 8.88 (s, 3H), 4.00 (s, 9H); ¹³C NMR (CDCl₃): 165.82, 135.00, 131.59, 53.03; MS m/z (FAB) 253 ([M + H]⁺); Anal. Calcd for C₁₂H₁₂O₆: C, 57.14%; H, 4.80%. Found: C, 57.18%; H, 4.82%.

1,3,5-Tribromo-trimethylbenzene (4). A quantity of 6.00 g (22 mmol) of lithium aluminum hydride was added to 600 mL of dry THF. Then, 15 g (59.5 mmol) of **4** in 600 mL of dry THF was added dropwise at room temperature under vigorous stirring and an atmosphere of N₂. After dropwise addition was completed, the mixture was heated to reflux for 24h. The excess of reducing agent was destroyed by slow addition of water, and the solvent was evaporated. Then, 450 mL of a 48% HBr solution and 750 mL of toluene were added and heated to reflux for 24 h. The organic layer was separated, and the aqueous portion was extracted several times with diethyl ether. The organic layers were combined and removed under reduced pressure. The crude material was purified through a short column of silica with a 1/1 mixture of *n*-hexane/toluene. The solvents were evaporated under high vacuum to afford 19.12 g (53.6 mmol, 90% yield) of **4**. ¹H NMR (CDCl₃): 7.36 (s, 3H), 4.46 (s, 6H); ¹³C NMR (CDCl₃): 139.45, 129.99, 32.62; MS m/z (FAB) 357 ([M + H]⁺); Anal. Calcd for C₉H₉Br₃: C, 30.54%; H, 2.54%. Found: C, 30.12%; H, 2.55%.

Tris-[2-(tosyl)-ethyl]-amine (5). Tris(2-aminoethyl)amine (4.83 g, 33.0 mmol) was dissolved in 70 mL of water containing 4.23 g (106 mmol) of NaOH. To this solution, *p*-toluenesulfonyl chloride (19.17 g, 100 mmol) in 60 mL of ether was added dropwise with vigorous stirring at room temperature. After the addition was complete, stirring

was continued for 2 h, and the reaction mixture was allowed to stand for 12 h. The white solid that precipitated was filtered, washed with copious amounts of water, and dried under high vacuum to afford **5** as a white powder (16.28 g, 26.7 mmol, 81% yield). ¹H NMR (CDCl₃): 7.78 (d, *J* = 8.3, 6H), 7.27 (d, *J* = 8.3, 6H), 5.96 (b, 3H), 2.90 (b, 6H), 2.48 (b, 6H), 2.40 (s, 9H); ¹³C NMR (CDCl₃): 143.70, 137.15, 130.18, 127.59, 54.55, 41.16, 21.92; MS *m/z* (FAB) 609 ([M + H]⁺); Anal. Calcd for C₂₇H₃₆S₃O₆N₄: C, 53.27%; H, 5.96%; N, 9.20%. Found: C, 53.31%; H, 5.89%; N, 9.15%.

3,3',3''-Tritosyl-6,6',6'-nitrilotri(3-azahexanenitrile) (6). A mixture of **5** (15.0 g, 24.6 mmol), acrylonitrile (5.3 mL, 81.3 mmol), K₂CO₃ (11.2 g, 81.3 mmol), and 200 mL of CH₃CN were heated at 70 °C and stirred for 3 days. Upon cooling, H₂O (1 L) and CHCl₃ (650 mL) were added, and the aqueous phase was washed with CHCl₃ (3 × 200 mL). The combined organic layers were dried under high vacuum, and the residue was recrystallized from MeOH/CHCl₃ to afford the product as white solid (16.6 g, 22.9 mmol, 93% yield). ¹H NMR (CDCl₃): 7.67 (d, *J* = 8.3, 6H), 7.28 (d, *J* = 8.3, 6H), 3.33 (t, *J* = 6.8, 6H), 3.20 (t, *J* = 6.8, 6H), 2.80 (t, *J* = 7.5, 6H), 2.63 (t, *J* = 6.7, 6H), 2.37 (s, 9H); ¹³C NMR (CDCl₃): 149.23, 140.94, 135.57, 132.68, 124.33, 58.52, 52.21, 50.51, 26.58, 23.72; MS *m/z* (FAB) 727 ([M + H]⁺); Anal. Calcd for C₃₆H₄₅S₃O₆N₇: C, 56.30%; H, 5.91%; N, 12.77%. Found: C, 56.22%; H, 5.85%; N, 12.70%.

3,3',3''-Tritosyl-6,6',6'-nitrilotri(3-azahexylamine) (7). **6** (7.27 g, 10 mmol) was dissolved in a solution of B₂H₆ in THF (200 mL, 1.0 M) and heated to reflux for 12 h under N₂. After cooling to room temperature, MeOH (30 mL) was added slowly to destroy excess B₂H₆, and the solvents were evaporated. The residue was dissolved in 2.5 M HCl/MeOH (300 mL) and refluxed for 3 h. The solvents were evaporated, the residue was partitioned between CHCl₃ (250 mL) and 1 M NaOH (150 mL), and the aqueous layer was extracted with CHCl₃ (2 × 150 mL). The organic layers were combined and dried under high vacuum to afford the crude amine as a viscous oil, which was used directly to the next step.

N,N',N''-3,3',3''-Hexatosyl-6,6',6'-nitrilotri(3-azahexylamine) (8). Compound **7** afforded directly from the previous step was dissolved in THF (150 mL)/CH₂Cl₂ (15 mL). To this mixture, Et₃N (15.6 mL, 112 mmol) and TsCl (6.23 g, 32 mmol) in 20 mL THF were added over 10 min, and the mixture was stirred for 12 h at room temperature. The solvents were evaporated, and the residue was partitioned between CHCl₃ and H₂O. The aqueous layer was extracted with CHCl₃ (2 × 150 mL), and the organic layers were combined and dried under high vacuum. The residue was purified by column chromatography on silica (CH₂Cl₂) to afford **8** as a powder (4.86 g, 4.5 mmol, 45% yield). ¹H NMR (CDCl₃): 7.77 (d, *J* = 8.3, 6H), 7.70 (d, *J* = 8.3, 6H), 7.39 (d, *J* = 8.3, 6H), 7.33 (d, *J* = 8.3, 6H), 2.99 (b, 6H), 2.91 (b, 6H), 2.75 (b, 6H), 2.48 (s, 9H), 2.46 (s, 9H), 0.87 (b, 12H); ¹³C NMR (CDCl₃): 144.04, 143.65, 137.12, 136.00, 130.32, 130.08, 127.58, 127.39, 54.33, 47.90, 47.49, 40.61, 29.35, 21.91, 21.89; MS *m/z* (FAB) 1228 ([M + H]⁺); Anal. Calcd for C₅₇H₇₅S₆O₁₂N₇: C, 55.72%; H, 6.15%; N, 6.84%. Found: C, 55.74%; H, 6.00%; N, 7.34%.

5,9,15,19,24,28-Hexakis-(toluene-4-sulfonyl)-5,9,12,15,19,24,28-heptaaza-tricyclo[10.10.8.1^{3,21}]hentriaconta-1(22),2,21(31)-triene (2). **8** (5.50 g, 4.48 mmol) and Cs₂CO₃ (80 g, 245.5 mmol) were suspended in refluxing CH₃CN (700 mL). To this mixture, a solution of **4** (1.60 g, 4.48 mmol) in CH₃CN (700 mL) was added dropwise. After the addition was complete, the suspension was refluxed and stirred for 36 h and then filtered. The solvent was removed, and the crude product was purified by column chromatography on silica (toluene/AcOEt, 85/15). The product was obtained as a white crystalline solid (1.13 g, 0.49

mmol, 19% yield). The same reaction performed with K₂CO₃ afforded only 11% yield. ¹H NMR (CDCl₃): 7.68 (d, *J* = 8.2, 6H), 7.62 (d, *J* = 8.2, 6H), 7.57 (s, 3H), 7.25 (m, 12H), 4.12 (s, 6H), 3.15 (b, 6H), 3.06 (b, 6H), 2.84 (b, 6H), 2.44 (b, 6H), 2.36 (s, 9H), 2.33 (s, 9H), 1.62 (b, 6H); ¹³C NMR (CDCl₃): 144.02, 143.74, 135.35, 134.78, 130.24, 130.14, 128.80, 128.38, 127.98, 127.60, 56.12, 55.41, 49.30, 48.96, 45.20, 27.73, 21.91; MS *m/z* (FAB) 1315 ([M + H]⁺); Anal. Calcd for C₆₆H₈₁S₆O₁₂N₇: C, 59.03%; H, 6.08%; N, 6.26%. Found: C, 59.20%; H, 6.19%; N, 6.39%.

5,9,12,15,19,24,28-Heptaaza-tricyclo[10.10.8.1^{3,21}]hentriaconta-1(22),2,21(31)-triene (1). A mixture of **2** (0.5 g, 0.38 mmol), phenol (2.0 g, 21.25 mmol), and 30 mL of 48% aqueous HBr was stirred and heated to reflux for 72 h. After cooling to room temperature, the mixture was repeatedly washed with chloroform. The aqueous phase was cooled to 0 °C, and sodium hydroxide was added slowly until the pH of the solution became at least 12. The product was extracted in chloroform, which was removed under high vacuum to afford the free amine as a waxy solid (80 mg, 0.19 mmol, 50% yield). ¹H NMR (CDCl₃): 7.20 (s, 3H), 3.84 (s, 6H), 2.63 (b, 12H), 2.57 (b, 12H), 2.40 (b, 6H), 1.53 (b, 6H); ¹³C NMR (CDCl₃): 141.78, 126.71, 54.23, 53.44, 49.04, 47.79, 47.41, 31.74; HRMS calcd for C₂₃¹³C₁H₄₅N₇Na [M + H]⁺, 455.3662; found, 455.3650.

Conclusion

Overall, it is concluded that complexation of a halide anion by the protonated cryptand **1** in the solid state follows the same pattern of distorted octahedral geometry, irrespective of the complexed halide and *irrespective of the nature of the donor groups*. The structural unit N(CH₂CH₂NH₂⁺CH₂CH₂CH₂)₃– plays a very important role in the binding of the halides in the newly synthesized cryptates.

Solution studies showed that basicity constants of **1** are in good agreement with those observed for related macrobicyclic azaphane species despite the unusual constraints placed on the geometry and donor atom set of **1**. Compound **1** in its hexaprotonated form displays high selectivity for fluoride over chloride (log *K*_{F⁻}/log *K*_{Cl⁻} > 5), whereas no binding in aqueous solution was found to take place for bromide and nitrate. An explanation for the existence of cryptate inclusion complexes of compound **1** in the solid state with bromide and iodide is probably its dramatic enhancement of affinity for halides (at least for bromide and iodide) at very low pH and concentration effects.

Acknowledgment. We thank King's College London and the EPSRC for funding for the diffractometer system, the Department of Chemistry at King's College London for a studentship (to C.A.I.), and the Nuffield Foundation for the provision of computing equipment. We also thank Professor Peter Gans (University of Leeds) for his advice on the usage of the program HYPERQUAD.³³

Supporting Information Available: X-ray structural data and plots of pH titration curves for the basicity determination of **1** and its binding of F⁻ and Cl⁻ (PDF, CIF). This material is available free of charge via the Internet at <http://pubs.acs.org>.

JA047070G